Non-Invasive Characterization of Breast Cancer Using Near Infrared Optical Spectroscopy

Ryan Lanning ~
Biological Sciences and Chemistry

Author

Ryan feels that his research experiences have helped pave the way toward his major goal of obtaining an M.D./Ph.D. and pursuing medical research as a career. He pursued his current research because of an interest in techniques for detecting, treating, and curing cancer. One of the perks of undertaking this project was the chance for Ryan to take apart, modify, and reassemble a very valuable instrument, as well as work with and learn from "many giants in the field." Ryan says that participating in research as an undergraduate has helped him acquire a sense of self-achievement, enriching the learning experience.

Key Terms:

- Absolute Absorption Coefficient (μ_a)
- Frequency-Domain Photon Migration (FDPM)
- Photon Density Waves (PDW)
- Reduced Scattering Coefficient (μ_s')
- Standard Diffusion Equation

Abstract

Breast cancer exists in a variety of disease states that cannot be easily characterized with current non-invasive diagnostic methods. This study presents possible methods for characterizing the disease states of breast cancer by analyzing their optical and physiological properties by frequency-domain photon migration (FDPM) techniques. A palpable breast lesion on four patients was measured using a high bandwidth (1-GHz) FDPM instrument utilizing six wavelengths spanning red and infrared light. The optical absorption (μ_a) and reduced scattering (μ_s') coefficients were calculated from the frequency dependence of the photon density waves (PDW). Using the optical absorption coefficients, the (oxy-, deoxy-, and total) hemoglobin concentration and water percentage were calculated. Statistical methods were applied to compare the optical parameters of the cancerous and normal tissue in each patient. Analysis of the statistical and physiological results of all the patients reveals an observable distinction among the different disease states of breast cancer.

Faculty Mentor

Pathologists routinely examine thin sections of surgically removed tissue in order to diagnose cancer. In this work, Ryan Lanning describes a new non-invasive diagnostic method, known as "photon migration," that employs near-infrared diode lasers to probe and analyze light scattered from tissues without surgical excision. This advanced technology allows us to measure the exact magnitude of light absorption and scattering (i.e. optical properties) *in vivo* without risk or discomfort to the patient. We show that photon migration can be taken from "bench-top to bedside" by developing a portable, state-of-the-art instrument and conducting clinical measurements on patients. These results demonstrate that tissue optical properties can be used to locate and identify physiological changes characteristic of both malignant and benign tumors in the breast. This is particularly important for young and "high risk" women who have radiographically dense tissue and typically do not benefit from conventional x-ray mammography.

~ Bruce Tromberg
College of Medicine
Beckman Laser Institute and Medical Clinic

Introduction

After lung cancer, breast cancer is the leading cause of cancer death in women and the leading cause of death for women between the ages of 40 and 55. Annually, approximately 44,000 women in the United States alone die from breast cancer, and estimates by the American Cancer Society predict about 175,000 cases in 1999. Present non-invasive detection methods for breast cancer cannot effectively characterize and diagnose the differences between malignant and benign tumors. In fact, the most effective method to date, x-ray mammography, presents a possible health risk by producing ionizing radiation. Studies have shown that a certain percentage of the population are genetically predisposed to the ionizing radiation of x-rays, increasing their risk of cancer induction (Klinteberg, 1999). Due to these effects, alternative diagnostic methods have been developed, including positron emission tomography, MRI, ultrasound, thermography, and various optical techniques. This study analyzes an optical technique, frequency domain photon migration (FDPM), as a possible non-invasive technique to determine the disease states of breast cancer.

In FDPM, the intensity of light incident upon an optically turbid sample is modulated at high frequencies (MHz-GHz), and the diffusely reflected or transmitted signal is measured with a phase-sensitive detector. Intensity modulated light propagates through tissue with a coherent front, forming photon density waves (PDW) (O'Leary et al., 1992; Fishkin and Gratton, 1993; Tromberg, et al., 1993). PDW dispersion is highly dependent on the optical properties of the tissue (Tromberg et al., 1995). Analytical solutions to the photon diffusion equation have been developed and are used to calculate the absolute absorption (μ_a) and reduced scattering (μ_s') parameters by comparing measurements of frequency-dependent PDW phase and amplitude to these model functions (Fishkin and Gratton, 1993; Arridge et al., 1992; Haskell et al., 1994; Patterson, 1995). The absorption parameter (μ_a) is a measure of the amount of light (photons) that is absorbed by light-active molecules (chromophores) in the media measured. In biological tissue, these chromophores are physiologically relevant biomolecules, such as hemoglobin (in blood), water, and fat. In humans, the absorption parameters at different wavelengths can be used to estimate physiological properties (total, oxy-, deoxyhemoglobin, and water content) of measured tissue (Fishkin et al., 1997; Tromberg et al., 1997). The reduced-scattering parameter (μ_s') is a measure of the amount of light (photons) diverted from its original direction into other directions (scattered) by various structures. Both cellular and extracellular components contribute to the scattering parameter in biological tissue. In humans, more dense or fibrotic tissue causes a higher μ_s', whereas lower parameters can be caused by fluid-filled cavities.

The development of techniques using the FDPM instrument for the characterization of breast cancer may provide instant diagnosis of malignant or benign tumors in the clinic. Previous FDPM techniques have been used to provide images of tumors with coarse resolution, but have not characterized the disease state (Franceschini et al., 1997). Benign conditions such as fibrocystic changes and fibroadenoma occur clinically in 50% of women and do not usually result in an increased risk of breast cancer in the absence of hyperplasia (Hindle, 1990). Unfortunately, in many of these cases the tumor is surgically removed due to the ambiguity of present detection methods (Hindle, 1990; Beam et al., 1996). On the other hand, a number of mammographic studies result in false-negative diagnoses, especially for pre-menopausal women (Bird et al., 1992; Joensuu et al., 1994; Kerlikowske et al., 1996) and women receiving estrogen replacement therapy (Laya et al., 1996). For these reasons, it is necessary to develop alternative methods to characterize and diagnose breast cancer in a more sensitive and accurate manner.

Materials and Methods

FDPM Instrument

A portable, high-bandwidth, FDPM instrument with multiple light sources was used in the study. It measures the frequency-dependence of the phase (Φ) and amplitude (A) of photon density waves (PDW) diffusing through tissue at a given source detector separation (ρ) and source wavelength (λ). The central component of the FDPM instrument is a network analyzer (Hewlett Packard) which is used to produce radio frequency (RF) output at frequencies ranging from 5 MHz to 1 GHz. The RF signal is combined with a direct current source using individual bias-tees and a RF switch. This combined signal is then directed sequentially into one of the different laser diodes. Each light source is coupled to an 8´8 optical switch (DiCon Instruments) by 100-μm diameter gradient-index optical fibers.

A source fiber carries light from the optical switch and projects it onto the tissue. An avalanche photodiode (APD) is used to detect the diffuse PDWs that propagate through the biological tissue. The source fiber, an APD, and a second optical fiber (that directs diffuse light to a separate self-contained APD) are located directly on a handheld probe with many possible combinations of two source-detector separations (ρ). The probe ends of the two optical fibers and the APD are placed in direct contact with the patient. For human subject studies, approximately 80 sec are needed for the measurement and visualization of the PDWs at all six wavelengths. A computer (Macintosh Quadra) using virtual instrument software (LabView, National Instruments) controls the network analyzer and optical and RF switches. The source-detector separations used in this study were 1.3 and 2.5 cm.

Patient Measurement

Non-invasive optical property measurements were made on four human subjects. The first patient was a 67 year-old post-menopausal female with a single palpable lesion buried 0.7 cm under the skin in the upper lateral part of the right breast. Histological examination following surgical biopsy revealed a 1.5´2´1 cm ductal carcinoma *in situ*. Patient 2 was a 62 year-old post-menopausal female with a single palpable lesion buried 12.6 mm under the skin of the upper outer part of the left breast. After a surgical biopsy, histological results revealed a 3.6´3.1´1.9 cm infiltrating ductal carcinoma. Patient 3 was a 21 year-old pre-menopausal female with a palpable mass of approximately 2 cm located 1 cm under the skin of the upper portion of the left breast. Needle biopsy revealed a benign fibroadenoma. Patient 4 was a 20 year-old pre-menopausal female with a palpable mass located in the right upper outer breast. A sonogram and needle biopsy revealed a 1.6´1.1´1.7 cm fibroadenoma buried about 1 cm beneath the skin.

FDPM measurements were made on each patient by gently placing the instrument probe on the skin. Figure 1 shows the side and top views of the placement of the source (S) and detector (D) fibers at different ρ (side) and the marked area measured on the breast (top). The side view exaggerates the distance between the probe and skin surface; there is continuous contact between the two during the measurements. Measurements were taken at marked 0, 5, and 10 mm intervals from the approximate center of the tumor (determined from sonograms) along each branch of the marked area. The probe was returned to the center and rotated 90 degrees for the transitions from branch to branch. This method gave 8 measurements away from the center and 4 at the center. Normal breast tissue data was acquired in a symmetric region of the non-diseased breast in the same fashion. A set of 12 data points for both tumor and normal tissue was acquired for each patient at all six wavelengths.

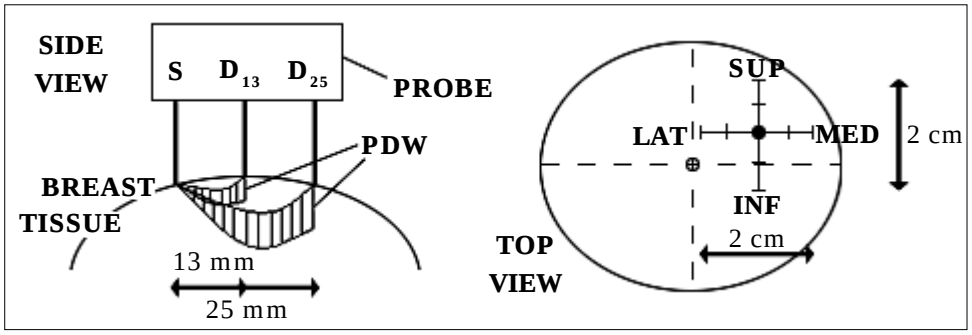

Figure 1

Side and Top views of the breast measurements. The side view shows the different depth the PDW samples at each ρ. The top view shows the marked measurements.

Data Analysis

The FDPM instrument recorded the average phase and amplitude data from 5 MHz to 1 GHz in 5 MHz increments. The data obtained was then fitted to model functions (Haskell et al., 1994; Fishkin et al., 1997) to obtain the absolute optical absorption coefficient (μ_a) and the absolute optical reduced scattering coefficient (μ_s') at each wavelength (λ) and source-detector separation (ρ). The χ^2 surface for a simultaneous fitting of the Φ and A versus frequency was minimized using a Marquardt-Levenberg algorithm. A tissue refractive index of 1.40 was assumed for all fits (Bolin et al., 1989).

The physiological properties that contribute to μ_a are principally oxy- and deoxyhemoglobin, and water (Cope, 1991; Sevick et al., 1991). Using the Beer-Lambert Law, the concentrations of each component contributing to μ_a can be calculated. A system of four equations of the form:

$$\varepsilon^{\lambda}_{[Hb]}[Hb] + \varepsilon^{\lambda}_{[HbO_2]}[HbO_2] + \varepsilon^{\lambda}_{[H_2O]}[H_2O] = \mu^{\lambda}_{\alpha}$$

were used, where $\varepsilon^{\lambda}_{[chrom.]}$ is the extinction coefficient (cm^2/mole) of a given chromophore at a specific wavelength. The extinction coefficients are obtained for the wavelengths 674, 803, 849 and 956 nm from literature values (Cope, 1991; Hale and Querry, 1973). Using a matrix representation of the four linear equations, the concentrations of the three unknowns can be calculated (Fishkin et al., 1997; Tromberg et al., 1997).

Statistical analysis was done on the optical properties for absorption and reduced scattering of each patient for comparison of diseased versus normal tissue. The variance at each wavelength was calculated over all the data points with the center measurements averaged. The variance was then calculated for only the center measurements. The relative standard deviation was calculated over all the data points with the center measurements averaged. A ratio of the normal to tumor relative standard deviation was calculated to provide an index for comparison among the different disease states of the cancer.

Results

The data collected at both 13 and 25 mm source-detector separations (ρ) provided similar values for both optical and physiological properties. The 13 mm separation provided results closer to normal tissue than the 25 mm due to the

PDW sampling closer to the surface of the tissue for shorter ρ. The diseased tissue in all patients had higher μ_a values relative to the normal breast tissue. For the scattering parameter, only patient 4 had higher m_s' values in the diseased tissue, while in patient 3 the μ_s' values were nearly equal. In patients 1 and 2, the diseased tissue had significantly lower scattering values than those in normal tissue. Due to the repetitive nature of the data, only the 25 mm results are presented.

An estimate of the spatial homogeneity of the tissue in the volume measured is given by the variance of both optical properties (μ_a and μ_s'), calculated for each set of measurements on diseased and normal tissues. The variance of both optical properties was greater in the diseased tissue than in the normal tissue for patients 1, 3, and 4. Patient 2 had higher variance in the normal breast than in the diseased breast for all of the wavelengths for μ_s' and some for μ_a. For both optical properties, patient 2 had the most

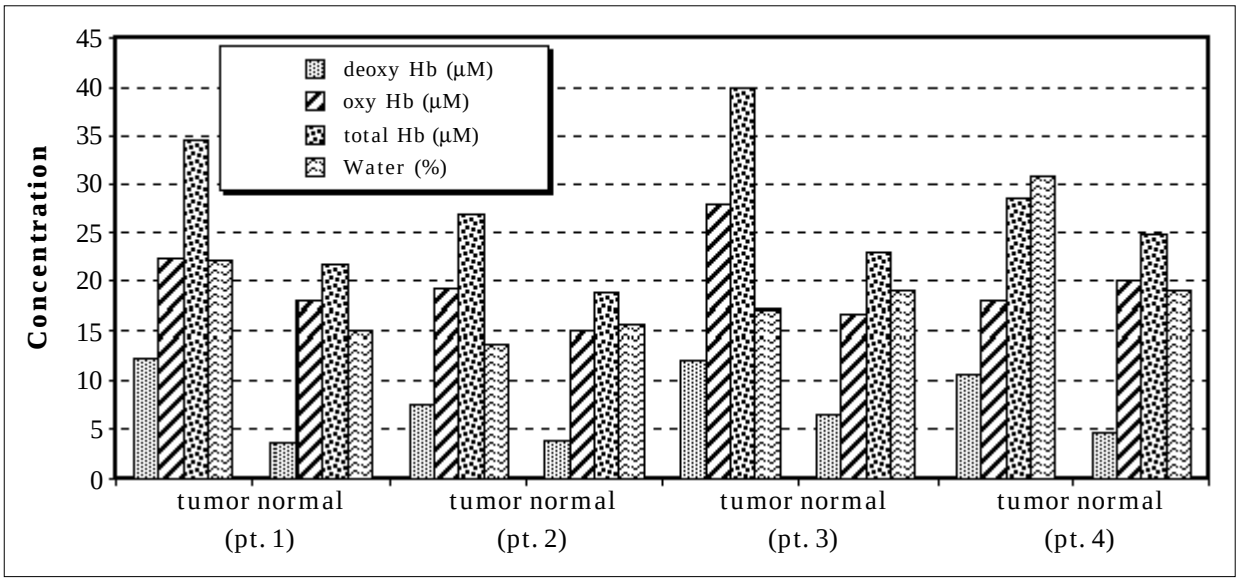

Figure 2

Hemoglobin (μM, deoxy-, oxy- and total) and water(%) for normal and tumor breast tissue, patients 1-4, calculated from wavelength-dependent μ_λ values.

The physiological data was calculated for each patient using the method described above and the m_a at 674, 803, 849, and 956 nm. The m_a data used in the calculations was the average of the four center measurements. The *in vivo* results of both the diseased and normal tissue are given in Figure 2 for all the patients. Total and deoxyhemoglobin levels are approximately two-fold higher in tumor versus normal tissue. Large oxyhemoglobin contrast occurs only in patient 3 (fibroadenoma). Differences in normal versus tumor tissue oxygen saturation (SaO_2) are significant for all but patient 3 (72% versus 79%, respectively). The SaO_2 values of patient 1 (83% versus 64%) and patient 4 (82% versus 63%) have the greatest separation followed by patient 2 (80% versus 71%). Normal SaO_2 values are comparable for all patients, except patient 3 (83%, 80%, 72%, and 82% for patients 1, 2, 3, and 4, respectively).

Tissue water percentage is also displayed in Figure 2. Patients 1 and 4 show a large contrast between normal versus tumor in the amount of water contained in the tissue (19% versus 31% and 15% versus 21%, respectively). There is approximately no contrast of normal versus tumor water percentage values for patients 2 and 3.

contrast between the normal versus tumor variance, followed by patient 1. Patient 3 showed the least contrast in variance between diseased and normal tissues.

The contrast for each patient is illustrated in Figure 3. The ratios depicted in the figure are the relative standard deviations for normal tissue versus tumor at each wavelength. The relative standard deviation is the standard deviation normalized by dividing by the average and provides a more direct way of comparing the variances between two sets of measurements. The top and bottom graphs illustrate the ratios for μ_a and μ_s', respectively. The closer the value is to 1, the smaller the contrast. Overall, patient 2 showed the greatest contrast, while patient 3 showed the least. The wavelengths in the 800 nm range appear to provide the most consistent results for the ratios in both μ_a and μ_s' for all patients. The results show a general pattern from the greatest to the smallest ratio. The order in both graphs is patients 2, 1, 3, and 4.

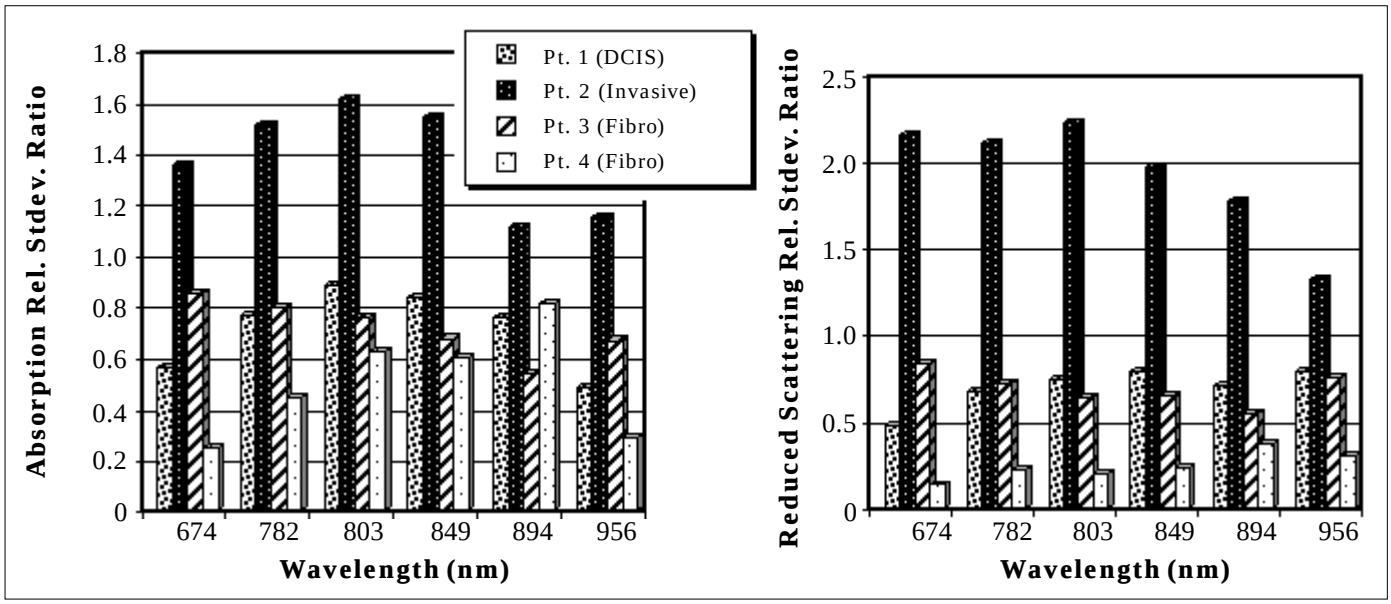

Figure 3

Ratio of normal versus tumor relative standard deviations as an index of the different disease states.

Discussion

The difference in the optical properties between the diseased and normal tissue parallels previous FDPM studies (Fishkin et al., 1997; Tromberg et al., 1997). The increased average absorption (μ_a) of the tumors is due to increased vascularity and in some cases, a larger concentration of water in the tumor itself. Scattering values are compatible with histology reports. A lower μ_s' is expected for fluid-filled structures with decreased cellularity (patients 1 and 2; DCIS and invasive DC, respectively) due to a decrease in the cellular components or tissue complexity that cause scattering. A higher μ_s' (patient 4) is expected in the case of fibrotic tissue (i.e., fibroadenoma) due to the dense and complex matrix of the tissue. Patient 3 had a μ_s' just below normal tissue values; this is possibly due to different optical properties in the area sampled by the FDPM probe. The values are still higher than those of patients 1 and 2, which suggests that it contained more fibrous tissue.

The most noticeable result in the calculated physiological properties (see Figure 2) is the increased total and deoxyhemoglobin in the diseased tissue of all patients. The increased vascular growth in tumors is the best explanation for these values. The increased concentration of deoxyhemoglobin is best analyzed by reviewing the tissue oxygen saturation (SaO_2) of normal versus tumor. Patients 1, 2, and 4 had a lower SaO_2 than normal tissue by significant amounts. Use of redox-sensitive probes has shown that tumor tissue is highly reducing (Kuppusamy et al., 1998). This reducing environment is due to increased metabolism in tumors and also explains the lower tissue oxygenation values. The higher SaO_2 value in patient 3 could be due to a benign tumor that is slow-growing, except that the normal tissue shows lower SaO_2 values than those of the other patients; therefore, there could be slight errors in these measurements. Thus far, the results for patient 3 demonstrate the smallest contrast between normal and diseased tissue, which would be consistent with earlier stage cellular differentiation.

The accuracy of the tissue water percentage values (see Figure 1) is difficult to confirm due to the fact that adipose tissue absorption was not taken into account (Tromberg et al., 1997). All results fall within the 11.4% to 30.5% range given by Duck (1990) for percentage water in human fatty adipose tissue. The only patients that show significant contrast are 1 and 4 (DCIS and fibroadenoma). It is possible that the DCIS contains a fluid-filled region and the matrix around the fibroadenoma contains increased water, which also corresponds with the high μ_a of both patients. The results from the other patients are inconclusive. The physiological properties are accurate enough to characterize a tumor from normal tissue but not accurate enough to characterize the different disease states of breast cancer.

The statistical results of the optical properties of each patient provide the best characterization of the different disease states. The higher variances of patients 1, 3, and 4 in comparison to their normal tissue can be explained by the disease states of their breast tumors. Patients 3 and 4 had the highest variances for both μ_a and μ_s' due to the heterogeneity of the fibrous tumor (i.e., fibroadenoma) in comparison to the surrounding normal tissue. The different cell phenotype of the tumor and the complex interaction of these tumorous cells with the surrounding normal tissue lends to this heterogeneity (Baish and Jain, 1998). Patient 1 has a ductal carcinoma *in situ* (DCIS) which is a

more homogeneous tumor in comparison to the fibroadenomas due to decreased cellular difference in the tumor. The tumor has not yet penetrated the basal membrane of the breast to invade the surrounding normal tissue. Thus, heterogeneity in the optical properties still exists due to the above reasons, but not to the same extent. The ductal carcinoma from patient 2 showed a much lower variance in its optical properties due to its invasive properties. The tumor broke the basal membrane and spread invasion foci into the surrounding normal tissue. This caused a merging of the optical properties of the normal and tumor tissue in the tissue surrounding the body of the tumor. The FDPM instrument measured the average values of the tissue, producing less variance in the optical properties over the entire area measured. The relative standard deviation graphs of normal tissue to tumor (see Figure 2) demonstrate the variance distinction between the different disease states of the patients. The ratio produces an index whereby the invasiveness and danger of the tumor can be estimated for both optical properties. The danger increases with increasing index values.

Conclusion

This study has demonstrated that non-invasive spectroscopic techniques using a multi-wavelength near-infrared FDPM instrument may provide a suitable alternative to present detection methods for breast cancer. The measured optical and physiological properties using this method suggest differences between the detectable various disease states of breast cancer. This supercedes present methods of breast cancer detection in its rapid non-invasive procedure, its lower cost, and its low risk.

Attempts to characterize different types of breast cancer using the index presented above should be further investigated by increasing the scope of the study to include many patients with a variety of breast cancer disease states. A separate study should also analyze the effects of lesion size on optical properties. A normal study should also be completed to produce an average value for pre- and post-menopausal women. This would increase the accuracy in characterizing the disease states for the ratio method. Pursuing these studies may increase the rate of development for a non-invasive method for the detection and characterization of breast cancer.

Acknowledgements

I would like to thank the members of the FDPM group for their assistance, support, and answering of all my questions: Tuan Pham, Joon You, Thorsten Spott, Andrew Berger, Dorota Jakubowski, Natasha Shah, Vasan Venugopalan, Albert Cerussi, and Debbie Gordon. Special thanks to Dr. Bruce Tromberg for giving me the opportunity to work on this project.

Works Cited

Arridge, S.R., M. Cope, and D.T. Delpy. "The theoretical basis for the determination of optical path lengths in tissue: temporal and frequency analysis." Physics in Medicine and Biology 37 (1992): 1531-1560.

Baish, J.W. and R.K. Jain. "Cancer, angiogenesis and fractals." Nature Medicine 4 (1998): 984.

Beam, C.A., P.M. Layde, and D.C. Sullivan. "Variability in the interpretation of screening mammograms by US radiologists. Findings from a national sample." Archives of Internal Medicine 156 (1996): 209-213.

Bird, R.E., T.W. Wallace, and B.C. Yankaskas. "Analysis of cancers missed at screening mammography." Radiology 184 (Sept 1992): 613-617.

Bolin, F.P., L.E. Preuss, R.C. Taylor, and R.J. Ference. "Refractive index of some mammalian tissues using a fiber optic cladding method." Applied Optics 28 (1989): 2297-2303.

Cope, M. The development of a near infrared spectroscopy system and its application for non invasive monitoring of cerebral blood and tissue oxygenation in the newborn infant. Diss. University of London, Department of Medical Physics and Bioengineering, University College London, 1991.

Duck, F.A. Physical Properties of Tissue. London: Academic Press, 1990.

Fishkin, J.B., O. Coquoz, E.R. Anderson, M. Brenner, and B.J. Tromberg. "Frequency-domain photon migration measurements of normal and malignant tissue optical properties in a human subject." Applied Optics 36 (1997): 10-20.

Fishkin, J.B. and E. Gratton. "Propagation of photon density waves in strongly scattering media containing an absorbing semi-infinite plane bounded by a straight edge." Journal of the Optical Society of America *A* 10 (1993): 127-140.

Franceschini, M.A., K.T. Moesta, S. Fantini, G. Gaida, E. Gratton, H. Jess, W.W. Mantulin, M. Seeber, P.M. Schlag, and M. Kaschke. "Frequency-domain techniques enhance optical mammography: Initial clinical results." Proceedings of the National Academy of Sciences *USA* 94 (1997): 6468-6473.

Hale, G.M. and M.R. Querry. "Optical constants of water in the 200 nm to 200 m wavelength region." Applied Optics 12 (1973): 555-563.

Haskell, R.C., L.O. Svaasand, T.T. Tsay, T.C. Feng, M.S. McAdams, and B.J. Tromberg. "Boundary conditions for the diffusion equation in radiative transfer." Journal of the Optical Society of America *A* 11 (1994): 2727-2741.

Hindle, W.H. Breast Disease for Gynecologists. New Jersey: Prentice Hall, 1990: 155-71.

Joensuu, H., R. Asola, K. Holli, E. Kumpulainen, V. Nikkanen, and L.M. Parvinen. "Delayed diagnosis and large size of breast cancer after false negative mammogram." European Journal of Cancer 30 (1994): 1299-1302.

Kerlikowske, K., D. Grady, J. Barclay, E.A. Sickles, and V. Ernster. "Effect of age, breast density, and family history on the sensitivity of first screening mammography." Journal of the American Medical Association 276 (1996): 33-38.

Klinteberg, C. On the use of light for the characterization and treatment of malignant tumors. Diss. Department of Physics, Lund Institute of Technology, 1999: 10.

Kuppusamy, P., M. Afeworki, R.A. Shankar, D. Coffin, M.C. Krishna, S.M. Hahn, J.B. Mitchell, and J.L. Zweier. "In vivo electron paramagnetic resonance imaging of tumor heterogeneity and oxygenation in a murine model." Cancer Research 58 (1998): 1562-1568.

Laya, M.B., E.B. Larson, S.H. Taplin, and E. White. "Effect of estrogen replacement therapy on the specificity and sensitivity of screening mammography." Journal of the National Cancer Institute 88 (1996): 643-649.

O'Leary, M.A., D.A. Boas, B. Chance, and A.G. Yodh. "Refraction of diffuse photon density waves." Physical Review Letters 69 (1992): 2658.

Patterson, M.S.. "Noninvasive measurements of tissue optical properties: Current status and future prospects. Comments on molecular and cellular biophysics." Comments on Modern Biology *A* 8 (1995): 387-417.

Sevick, E.M., B. Chance, J. Leigh, S. Nioka, and M. Maris. "Quantitation of time- and frequency-resolved optical spectra for the determination of tissue oxygenation." Analytical Biochemistry 195 (1991): 330-351.

Tromberg, B.J., L.O. Svaasand, T-T. Tsay, and R.C. Haskell. "Properties of photon density waves in multiple scattering media." Applied Optics 32 (1993): 607-616.

Tromberg, B.J., R.C. Haskell, S.J. Madsen, and L.O. Svaasand. "Characterization of tissue optical properties using photon density waves." Comments on Molecular Cell Biophysics 8 (1995): 359-386.

Tromberg, B.J., O. Coquoz, J.B. Fishkin, T. Pham, E.R. Anderson, J. Butler, M. Cahn, J.D. Gross, V Venugopalan, and D. Pham. "Non-invasive measurements of breast tissue optical properties using frequency-domain photon migration." Philosophical Transactions of the Royal Society of London *B* 352 (1997): 661-668.